JOURNAL OF VIROLOGY, Apr. 1992, p. 2378–2388
0022-538X/92/042378-11$02.00/0

Vol. 66, No. 4

Homologous Recombination of Copackaged Retrovirus RNAs during Reverse Transcription

HEIDI STUHLMANN†* AND PAUL BERG

Department of Biochemistry, Beckman Center, Stanford University School of Medicine, Stanford, California 94305-5307

Received 2 October 1991/Accepted 14 January 1992

According to prevailing models, the high frequency of recombination in retroviruses occurs during reverse transcription of two genetically different genomes copackaged into virion particles. This view has been tested in our studies of the mechanism of recombination within homologous sequences of two retroviral genomes during a single round of virus replication and in the absence of helper virus. The recombination substrates were Moloney murine leukemia virus-based vectors, each of which contains an altered defective neomycin gene (*neo*) under the transcriptional control of the 5′ long terminal repeat; the 3′ sequences of each construct contain either the Moloney murine leukemia virus or simian virus 40 large-T polyadenylation sequence. One *neo* gene contained a linker insertion mutation at the 5′ end (*neo* minus), and the other contained a deletion and linker insertion at the 3′ end ($neo^{\Delta 3}$). Each of the mutant *neo* constructs was introduced into the packaging helper cell line Ψ2 by sequential cotransfection, and individual Ψ2 double transformants were selected. Supernatant fluids from the cloned Ψ2 double transformants were used to infect NIH 3T3 cells, and recombinant neo^+ proviruses were detected by their ability to confer G418 resistance during infection of NIH 3T3 cells. Our results show that (i) recombination between a homologous sequence of about 560 bp occurred with a frequency of about 10^{-4} per virus replication cycle; (ii) recombination occurred only after the viral RNAs had been packaged into particles, i.e., recombination between the two vector DNAs or between viral RNAs prior to packaging was not detected; and (iii) copackaging of two different genomic RNAs as a heterodimer is a prerequisite for recombination. Furthermore, our results indicate that recombination can occur during the DNA negative-strand synthesis of reverse transcription.

Recombination between retrovirus genomes was first demonstrated during mixed infections with genetically marked avian tumor viruses (4, 18, 32, 36, 37) and murine leukemia viruses (10, 35) and, more recently, with human retroviruses (7). Moreover, exogenous viruses can recombine with endogenous retroviral sequences (9, 28, 34), giving rise to viruses with expanded host range properties. It is also well established that retroviruses can recombine with cellular sequences to give rise to transforming viruses (for an overview, see reference 19).

One of the unusual features of retroviral recombination is that the frequency of genetic exchanges that occur during mixed infections with either avian or murine retroviruses is very high compared to other RNA viruses (4, 18, 35, 36). A clue to the origin of such frequent exchanges emerged from the recognition that RNA rather than DNA molecules are the substrates for recombination between avian tumor viruses (34). Another significant feature of retroviral recombinations is that they do not appear within a single round of infection, i.e., from the initially mixedly infected cells; rather, they appear only after a second infection by the progeny of the initially infected cells. This unusual characteristic stems from the diploid nature of the virion genome and its mode of replication. Thus, retrovirus genomes consist of two RNA positive strands which are held together in mature virion particles at or near their 5′ ends (1, 2, 23, 24). Consequently, it seems likely that virions produced initially after mixed infections contain RNA strands corresponding to each of the infecting viruses and that genetic exchanges occur only after a second infection by the heterozygous virions. Genetic data are consistent with the occurrence of heterozygous virions (29, 34, 36, 37), but physical evidence for their existence is lacking.

Two models have been proposed to account for genetic exchanges during infection of cells with genetically distinctive retroviruses; both require the formation of heterozygous virions in the initially infected cells and genetic exchanges during reverse transcription in subsequently infected cells. The two models differ in how and when the genetic exchanges are presumed to occur. Coffin (8) proposed a modified copy choice mechanism in which reverse transcriptase switches from one RNA template to another upon encountering breaks in the RNA strands. The alternative model, proposed by Junghans et al. (17), assumes that the two RNA genomes are each reverse transcribed into negative-strand DNA and that single-stranded DNA branches are formed and recombine with homologous regions on the other cDNA in a displacement-assimilation mechanism. Recent experimental evidence implicating heterozygous virions (14) and reverse transcriptase (12, 30) is consistent with both models. Support for the copy choice model has been provided by experiments showing that reverse transcriptase can switch to a second RNA strand after reverse transcribing to the end of an RNA template in vitro (20).

The copy choice and displacement-assimilation models for reverse transcriptase-mediated recombination make specific predictions, some of which can be tested experimentally. For example, according to the copy choice model, the recombination between heterodimeric RNA templates takes place during DNA negative-strand synthesis and always leads to a single recombinant provirus (8). In contrast, the

* Corresponding author.
† Present address: Brookdale Center for Molecular Biology, Mount Sinai School of Medicine, New York, NY 10029.

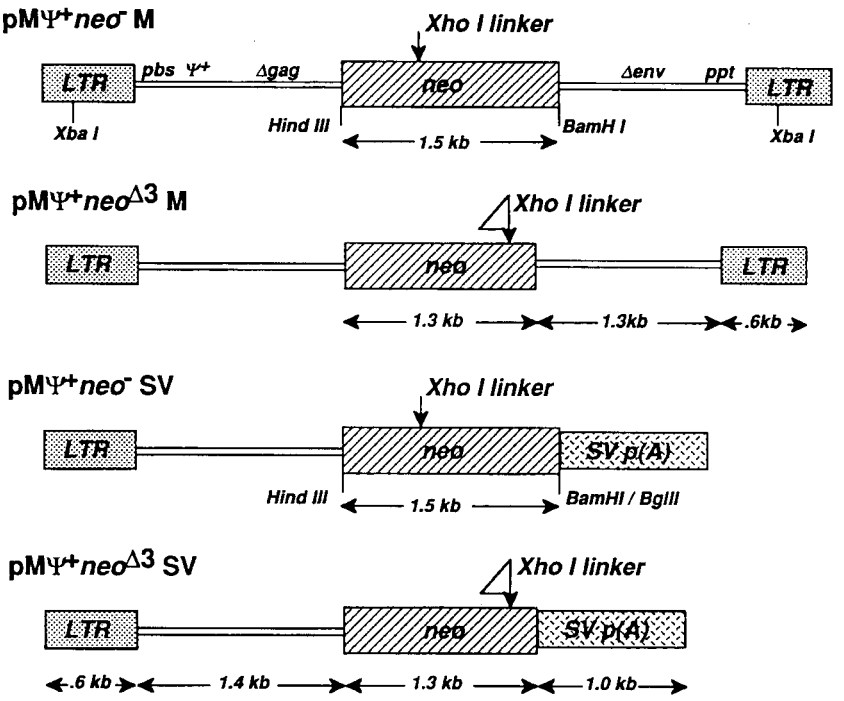

FIG. 1. Structure and derivation of mutant *neo* vectors. These vectors contain a bacterial *neo* gene with either *Xho*I linker insertions in the 5′ region (*neo* minus), or a 180-bp deletion and *Xho*I linker insertion at the 3′ end ($neo^{\Delta 3}$) (26). The vectors contain 5′ MoMLV sequences up to nucleotide 1560 (33); these include the 5′ LTR, the primer- binding site (*pbs*), the packaging site Ψ, and 995 bp of *gag* sequences. The 3′ sequences are derived either from MoMLV and include 1,240 bp of *env* sequences, the polypurine tract (*ppt*), and the 3′ LTR, or from a 1-kb fragment containing the SV40 large T polyadenylation site [SVp(A)]. Some restriction sites used in the construction of the *neo* vectors are shown. The lengths of the fragments relevant to the analysis of the genome structures are indicated for the various regions of the constructs. Symbols: ▭, LTR; ═, MoMLV DNA sequences; ▨, *neo* gene; ▩, SV40 sequences.

assimilation-displacement model assumes that recombination takes place during the second, DNA positive-strand synthesis, the result being a parental-recombinant heteroduplex DNA, in which one strand is parental and the other is recombinant.

Recently we showed that infection of cells expressing a cell-like *neo* mRNA with a replication-competent Moloney murine leukemia virus (MoMLV) generated *neo* transducing virions (30). Our data indicated that *neo*-containing proviral genomes were formed by a reverse transcriptase-mediated recombination following infection with virions containing the two types of RNA. In the present report, we focus on the recombination between two defective *neo* sequences contained in MoMLV-based retroviral genomes during a single round of virus replication in the absence of helper virus. Our present results further support the contention that copackaging of genetically different RNAs is a prerequisite for recombination and that recombination occurs during DNA negative-strand synthesis by reverse transcription. The recombination frequency between two markers, which are 560 nucleotides apart, was ca. 10^{-4}.

MATERIALS AND METHODS

***neo* vector constructs.** A series of replication-defective, MoMLV-based vectors were constructed as substrates for recombination (Fig. 1). The constructs contain a 1,450-bp fragment (*Hin*dIII-*Pst*I) of the neomycin gene (*neo*) with mutations in the *neo* coding sequence (26). The 5′ mutation (*neo* minus) contains multiple *Xho*I linker fragments inserted at the *Pvu*II restriction site at position 585 of the *neo* coding sequence; the 3′ mutation ($neo^{\Delta 3}$) contains a 180-bp deletion 5′ of the *Sma*I site at position 1320 and a *Xho*I linker insertion at this site. The two *Xho*I restriction sites marking the mutations are 560 bp apart (26). The *neo* genes are transcribed from the 5′ long terminal repeat (LTR) promoter of MoMLV. In addition, all constructs contain 5′ MoMLV sequences derived from pMov 9 (6); these include sequences which are necessary for efficient packaging of genomic RNA (Ψ) and for initiation of negative-strand DNA synthesis during reverse transcription (*pbs*) and about 1 kb of *gag* sequences (Δ*gag*) up to the *Xho*I site at position 1560 (33). One set of the *neo* vectors contains a 3′ end consisting of MoMLV sequences from nucleotide 6537 derived from pMov 9, including the polypurine tract (*ppt*) for initiation of positive-strand DNA synthesis ($pM\Psi^+neo^-M$, $pM\Psi^+neo^{\Delta 3}M$); the other set has a 3′ end consisting of a 1-kb *Bcl*I-*Eco*RI fragment containing the simian virus 40 (SV40) large-T polyadenylation site ($pM\Psi^+neo^-SV$, $pM\Psi^+neo^{\Delta 3}SV$). Derivatives from these constructs containing a 350-bp deletion of the Ψ sequences (Ψ^-) (22) were also generated (not shown in Fig. 1).

Cell culture and virus infection. Ψ2 cells were obtained from R. C. Mulligan, Whitehead Institute, Cambridge, Mass. NIH 3T3, Ψ2, and XC cells were maintained in Dulbecco modified Eagle medium supplemented with 10% calf serum, penicillin, and streptomycin. Electroporation of Ψ2 cells was performed by the method of Chu et al. (5) with modifications

as described previously (30). About 48 h after electroporation, cells were transferred at a 1:20 dilution into selection medium. Ψ2 single transformants were generated by cotransfection with pSV2*dhfr** plasmid DNA (31) and selection in Dulbecco modified Eagle medium supplemented with 10% dialyzed calf serum and 0.3 μM methotrexate (Lederle Lab.). Ψ2 double transformants were produced by a second cotransfection with pSV2*his* plasmid DNA (13) and selection in Dulbecco modified Eagle medium supplemented with 10% calf serum and 2.5 mM L-histidinol (Sigma). Drug-resistant clones were isolated 10 days later and grown up for further analysis.

Culture supernatant from Ψ2 single and double transformants was harvested and filtered through sterile filters (Syrfil-MF [pore size, 0.45 μm]; Nucleopore Corp.). To test for formation of recombinant *neo*$^+$ virus, 5 ml of supernatant from Ψ2 double transformants was used to infect 10^6 NIH 3T3 cells (seeded the day before in culture medium supplemented with 4 μg of polybrene per ml). When cells were given a mixed infection with viruses from two different Ψ2 single transformants, 5 ml of supernatant from each were mixed with 10^6 NIH 3T3 cells. Two days after infection, the NIH 3T3 cells were trypsinized and divided onto two large petri dishes (diameter, 14 cm) with culture medium supplemented with 0.5 mg of G418 per ml. G418-resistant NIH 3T3 clones were isolated 10 days later and grown up for further analysis. Individual clones were tested for production of infectious recombinant *neo*$^+$ virus as well as for wild-type MoMLV by an XC plaque assay (25) before and after superinfection with MoMLV helper virus as described previously (30).

DNA preparation and Southern analysis. The preparation of high-molecular-weight DNA, agarose gel electrophoresis, and Southern hybridization were performed by standard procedures (21), using supported nitrocellulose membranes (BA-S NC; Schleicher & Schuell). A 1.5-kb *Bam*HI-*Hin*dIII *neo* fragment from pBR*neo* (27), which was used as a hybridization probe, was labeled with [α-^{32}P]dCTP by using the hexamer method (11).

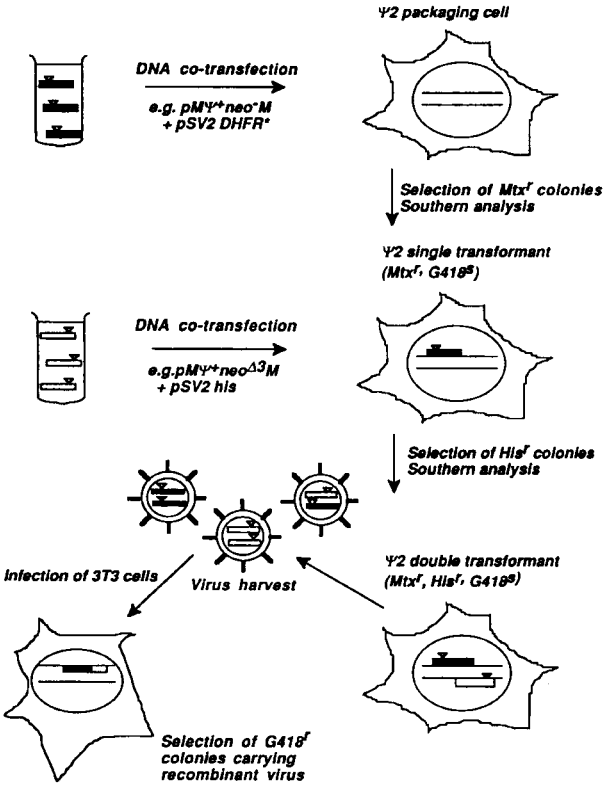

FIG. 2. Experimental scheme. DNA from two mutant *neo* constructs was introduced into the Ψ2 packaging cell line (22) by sequential cotransfections with dominant selectable markers. Ψ2 double transformants produce virions containing either identical RNAs from either of the two constructs or one each of the two RNAs. The latter virions are the presumed precursors for the formation of recombinant provirus, which can be selected for after infection of NIH 3T3 cells and selection for G418 resistance.

RESULTS

Experimental design for detecting *neo*$^+$ recombinant virus. The experimental scheme for monitoring recombination between homologous sequences of two retroviral genomes within one round of virus replication is outlined in Fig. 2. Combinations of two constructs, each carrying a different mutant *neo* gene (Fig. 1), were introduced by sequential cotransfection into the helper virus-free packaging cell line Ψ2 (22). This cell line provides all of the functions necessary for encapsidation of a retrovirus vector. The mutations are marked by unique *Xho*I linker insertions in the 5′ (*neo*-minus) or 3′ (*neo*$^{\Delta 3}$) region of the *neo* coding sequence and are 560 bp apart. The formation of recombinant *neo*$^+$ virus during the next virus replication cycle was monitored by infection of fresh fibroblast cells and selection for G418 resistance.

First, DNA constructs containing the *neo*-minus mutant gene were introduced into Ψ2 cells by cotransfection with pSV2*dhfr** which contains a mutant *dhfr* cDNA as a dominant selectable marker (31). Methotrexate-resistant (Mtx^r) clones (Ψ2 single transformants) were collected, and two independent clones that contained authentic copies of the *neo*-minus construct were cotransfected with DNA constructs containing a *neo*$^{\Delta 3}$ gene and pSV2*his* (13). Selected histidinol resistant (His^r) clones (Ψ2 double transformants) were analyzed for the presence of intact *neo*$^{\Delta 3}$ genomes by Southern blotting. Two Ψ2 double transformants derived from each Ψ2 single transformant clone and carrying one to three authentic copies from each construct were selected for further experiments.

Culture supernatant from G418-sensitive (G418^s) Ψ2 double transformants was harvested and used for infection of NIH 3T3 fibroblasts. These culture supernatants should contain three types of virus particles: ones carrying two identical virus genomes from either one of the two parental constructs, and ones containing a heterodimer with RNAs from each of the two parental genomes. NIH 3T3 clones with *neo*$^+$ recombinant proviruses were selected 2 days later by seeding the cells into G418 selection medium.

Recombination during one round of virus replication. Four Ψ2 double transformants, each carrying a different combination of two defective *neo* viruses, with one or few copies of each (shown in Fig. 1), were established (Fig. 3); each pair of constructs contains the 5′ mutation (*neo* minus) on one transcript and the 3′ mutation (*neo*$^{\Delta 3}$) on the other. A Ψ2 single transformant containing a retrovirus construct with a wild-type *neo* gene (MΨ$^+$*neo*$^+$M) was used as positive control. Viral RNA produced from the latter construct requires only packaging but not recombination to give rise to G418^r clones upon infection of NIH 3T3 cells.

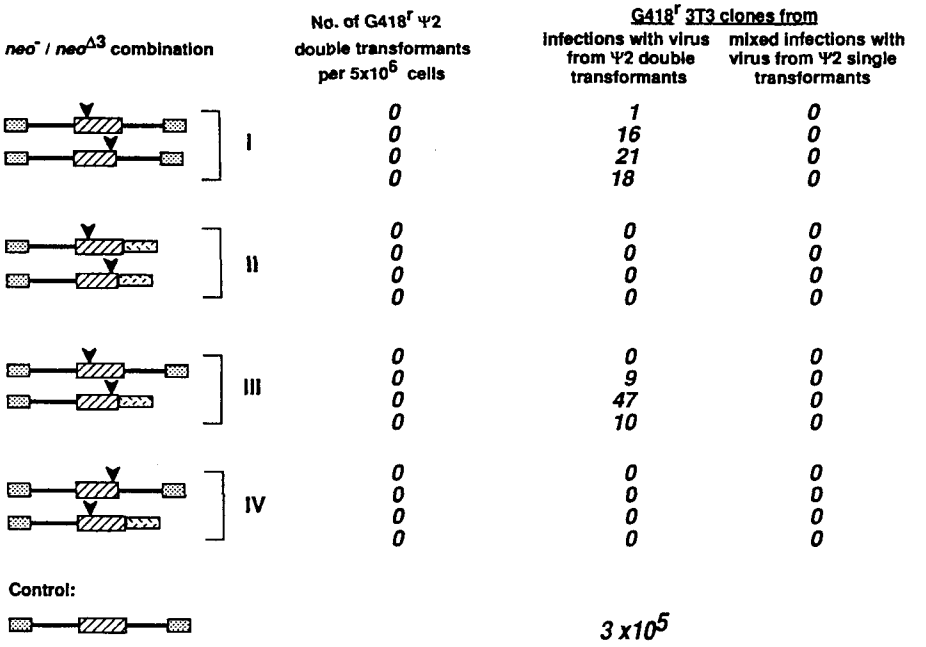

FIG. 3. Formation of recombinant *neo*$^+$ virus. The number of G418^r cells in various Ψ2 double-transformant clones carrying combinations of the *neo*-minus and *neo*$^{\Delta 3}$ vectors (left) is indicated in the first column. The number of G418^r clones formed following infection of NIH 3T3 cells with 5 ml of supernatant from cultures of the various Ψ2 double transformants is shown in the second column. The control titer was determined by infection of NIH 3T3 cells with 5 ml of supernatant from a Ψ2 clone transformed with a pMΨ$^+$*neo*$^+$M construct. The third column shows the number of G418^r clones formed when pooled supernatants from single transformants with the genomes shown at the left were used to infect NIH 3T3 cells. Four independent Ψ2 clones from each combination were analyzed. Symbols are as in Fig. 1.

To determine whether recombination between the two integrated mutant *neo* genes occurred in the doubly transformed cell lines or whether the Ψ2 cells had been reinfected with a recombinant *neo*$^+$ virus, approximately 5×10^6 cells from each clone were seeded in G418 selection medium. Figure 3, column 1, shows that there were no *neo*$^+$ cells in any of the selected doubly transformed Ψ2 lines. Southern blots from each of the doubly transformed clones confirmed that none of them contained cells with an intact *neo* sequence (<0.1 copy per cell [data not shown]).

Since the *neo* vectors are replication defective, their packaging into virions requires viral proteins provided in *trans* by the Ψ2 packaging cell line. Therefore, infection of NIH 3T3 cells with virus culture supernatants from the doubly transformed Ψ2 clones and subsequent G418 selection scores recombinant *neo*$^+$ proviruses generated within a single virus replication cycle. Moreover, because the virus-producing cells do not contain an intact *neo* sequence, any *neo*$^+$ recombinants must arise in the course of the infection, most probably by reverse transcriptase-mediated recombination between the mRNAs transcribed from the two mutant *neo* constructs following their encapsidation into virions (30).

A single homologous recombination during reverse transcription of the viral genomes in combinations I and III (Fig. 3) could generate *neo*$^+$ provirus DNA which is integration competent. With both combinations, the first strand transfer during DNA negative-strand synthesis could be either inter- or intramolecular and would continue on the viral 3′ terminus of the mutant *neo*-minus genome (upper transcript). As shown in Fig. 3, column 2, all four of the Ψ2 double-transformant clones carrying DNA from combination I gave rise to virus particles that were able to transduce G418^r to the recipient NIH 3T3 cells. Similarly, three of the four Ψ2 clones from combination III also transduced G418^r to the infected cells. Therefore it appears that a single recombination event between two replication-defective vectors can be detected within one round of virus replication.

In attempting to estimate the recombination frequency, we assume that the genomic RNAs containing mutant *neo* genes are packaged with the same efficiency as the RNA derived from the control pMΨ$^+$*neo*$^+$M construct; furthermore, we assume that there is no discrimination between the two different viral RNA genomes during packaging into virions. Under these conditions, half of the virus particles produced from a Ψ2 double transformant should contain heterodimer RNAs. However, because each Ψ2 double transformant carries the two defective *neo* genomes at different chromosomal integration sites, their expression may yield different amounts of genomic RNAs, thereby reducing the number of heterozygous virions. This variability would very probably influence the measured recombination frequency and yield different estimates among independent Ψ2 double transformants. On the basis of the number of recombinants obtained (Fig. 3), the recombination frequency within the 560 bp of homology between two retrovirus genomes was in the range of 1×10^{-5} to 3×10^{-4} per round of virus replication.

Virus supernatants from Ψ2 double transformants in which both mutant *neo* constructs contained SV40-derived 3′ termini (Fig. 3, combination II) were unable to generate *neo*$^+$ proviruses upon infection of NIH 3T3 cells. This is not surprising because both constructs lack the 3′ sequences needed for the first DNA negative-strand transfer, as well as the *ppt* sequence necessary for initiation of DNA positive-

TABLE 1. Production of *neo*$^+$ transducing virus from G418^r 3T3 clones[a]

G418^r 3T3 clone[b]	Virus production[c]			
	Without MoMLV		With MoMLV	
	wt virus (XC plaques)	*neo*$^+$ virus (G418^r clones/ml)	wt virus (XC plaques)	*neo*$^+$ virus (G418^r clones/ml)
Combination I				
A	+	3×10^0	+	1×10^0
B	−	−	+	3×10^4
C	−	−	+	1×10^4
D	−	−	+	3×10^4
E	−	−	+	1×10^4
F	−	−	+	1×10^4
G	−	−	+	4×10^4
H	−	−	+	2×10^4
Combination III				
A	−	−	+	2×10^4
B	−	−	+	3×10^4
C	−	−	+	ND[d]
D	−	−	+	2×10^4
E	−	−	+	3×10^4
F	−	−	+	1×10^4
G	+	6×10^0	+	6×10^0
H	−	−	+	20×10^0

[a] Eight G418^r 3T3 clones derived from infection with virus obtained from Ψ2 double transformants containing combination I or combination III were analyzed for spontaneous production of wild-type MoMLV virus and for the production of MoMLV and *neo*$^+$ virus following superinfection with MoMLV as described previously (30).

[b] Combination I, MΨ$^+$*neo*$^-$M/MΨ$^+$*neo*$^{\Delta 3}$M; combination III, MΨ$^+$*neo*$^-$M/MΨ$^+$*neo*$^{\Delta 3}$SV.

[c] Wild-type (wt) virus production was assayed by the XC plaque assay (25). Symbols: +, >10^5 XC PFU/ml; −, no detectable XC plaques. The titer of recombinant *neo*$^+$ virus was determined from the number of G418^r colonies produced after infection of NIH 3T3 cells. Symbol: −, no G418^r clones.

[d] ND, not done.

strand synthesis. Furthermore, even if reverse transcription could proceed, a *neo*$^+$ recombinant would fail to integrate since it lacks 3′ LTR sequences. Ψ2 clones carrying mutant *neo* constructs, as shown in Fig. 3, combination IV, did not produce any recombinant *neo*$^+$ viruses. In this case, two recombination events within one virus replication cycle would be required to generate a *neo*$^+$ recombinant provirus; the first is between the 3′ deletion site and the SV40 polyadenylation site, and the second is between the two *Xho*I markers in the *neo* sequence. If such double recombinations occur, their frequency seems to be too low to be detected in our assay.

G418^r NIH 3T3 clones arising by infection with virus derived from the Ψ2 double transformants should not produce *neo*-transducing virus spontaneously because they lack the information for forming infectious virus. However, both wild-type and *neo*-transducing virus should be produced after infection of such clones with MoMLV. That is, in fact, the result with seven of eight G418^r clones examined from combination I and seven of eight from combination III (Table 1). This further supports our notion that *neo*$^+$ virus was generated by a single homologous recombination between the two markers. We surmise that wild-type provirus DNA was generated in clone A from combination I and clone G from combination III, either by recombination (only one is needed) between an inadvertently packaged Ψ$^-$ MoMLV genome and either of the defective *neo* RNAs, or by superinfection of the G418^r 3T3 clone with a recombined Ψ$^+$ MoMLV. Evidently, the recombination events that led to the formation of the *neo*$^+$ alleles in clones A and G, and also in clone H, created a rearrangement that impaired the ability of the *neo*$^+$ sequences to be transduced after superinfection with MoMLV (Table 1).

Copackaging into heterozygous particles is a prerequisite for recombination. The *neo*$^+$ recombinant proviruses detected after one round of virus replication could have originated either from infection with a heterozygous virus particle containing two genetically different copackaged viral genomes, or from coinfection of the same cell with two virus particles each containing a homodimeric RNA. To distinguish between these possibilities, we mixed virus obtained from Ψ2 single transformants, each carrying only one of the mutant *neo* constructs shown in Fig. 1; each of these transformants produces virus with only homodimeric RNA. No G418^r recombinants were detected in such infections (Fig. 3, column 3).

The failure to detect *neo* transduction by mixed infection with viruses containing only homodimeric RNA might be because the virus titers produced by the Ψ2 single transformants were too low for efficient double infection of the 3T3 cells. Because the viruses produced by the single transformants lack a functional *neo* gene, it was not possible to determine their titers directly. Assuming that the single transformants produce an amount of virus equivalent to the 10^5 *neo*-transducing particles per ml released by Ψ2 cells transformed with MΨ$^+$*neo*$^+$M (Fig. 3), the 5 ml of each supernatant used to infect 2×10^5 NIH 3T3 cells would correspond to a multiplicity of infection of ca. 2.5. Using the Poisson equation, which estimates the sampling distribution for the fraction of cells receiving *n* virions as a function of the multiplicity of infection, the probability that a cell is infected with two viruses containing each of the two *neo* alleles is 0.84 for a multiplicity of infection of 2.5 and 0.4 for a multiplicity of infection of 1. In addition, 20-fold concentration of virus supernatants before mixed infections did not yield *neo*-transducing viruses (data not shown). Therefore, we conclude that most cells were infected by viruses containing each of the two *neo* alleles. This supposition is further supported by the finding that the cellular DNA from most G418^r 3T3 clones contains more than one provirus (see below).

Structure of *neo* recombinant proviruses. The structure of the recombinant proviral DNAs and the proviral integration sites were examined by Southern blotting analysis of restriction endonuclease digests of the cellular DNA from G418^r 3T3 clones. The most informative cleavage sites, shown at the bottom of Fig. 4, were those of *Xba*I, which cleaves once in each LTR, and *Xho*I which cuts the DNA at the mutation sites in the *neo* gene. Digests obtained with both enzymes together yield *neo*-containing fragments of 2.3 and 2.5 kb from MΨ$^+$*neo*$^-$M DNA, 2.9 and 1.7 kb from MΨ$^+$*neo*$^{\Delta 3}$M DNA, and 4.8 kb from a provirus containing a wild-type *neo* sequence (Fig. 4, bottom). Cleavage of the proviral form of MΨ$^+$*neo*$^{\Delta 3}$SV with the same pair of enzymes yields a 2.9-kb *neo*-containing fragment (Fig. 5, bottom). Digestion with *Hin*dIII, which cuts at the 5′ border of the *neo* gene, generates a fragment characteristic for the 3′-flanking sequences at the provirus integration site.

Homologous recombination during reverse transcription of RNAs derived from combination I or III should generate a *neo*$^+$ provirus which has lost both *Xho*I restriction sites. Therefore, double digestion with *Xba*I and *Xho*I should yield the 4.8-kb fragment produced by analogous digestion of

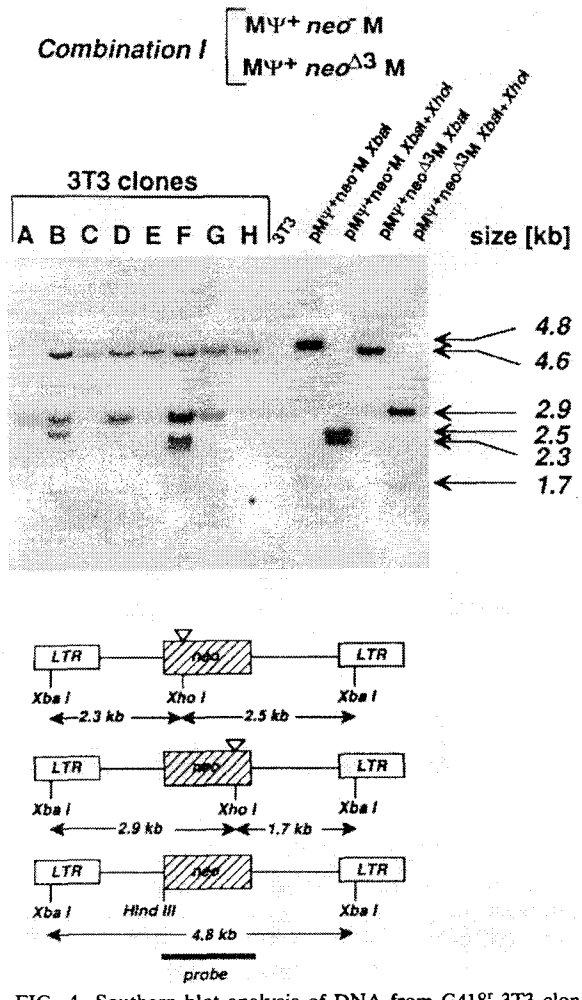

FIG. 4. Southern blot analysis of DNA from G418^r 3T3 clones infected with virus from combination I (MΨ^+*neo*$^-$M/MΨ^+*neo*$^{\Delta 3}$M). High-molecular-weight DNA (10 μg) was digested to completion with *Xba*I and *Xho*I, separated on 1% agarose gels, and transferred to BA-S NC filters. λ DNA, digested with *Eco*RI and *Hin*dIII, was run in parallel to provide size markers. The filters were hybridized with 10^7 cpm of an α-^{32}P-labeled 1.5-kb *neo* fragment. (Top) *Xba*I-*Xho*I endonuclease digests. Lanes: A to H, 10 μg of DNA from eight different G418^r 3T3 clones; 3T3, 10 μg of NIH 3T3 DNA. As controls, 10 μg of NIH 3T3 DNA mixed with 10 pg of pMΨ^+*neo*$^-$M DNA or with 10 pg of pMΨ^+*neo*$^{\Delta 3}$M DNA was digested with *Xba*I endonuclease alone or with *Xba*I and *Xho*I as indicated. The sizes of the respective fragments are indicated. (Bottom) Schematic structures of the mutant *neo* constructs and the putative recombinant *neo*$^+$ provirus. The positions of the *Xba*I, *Xho*I, and *Hin*dIII cleavage sites, the sizes of the expected fragments, and the probe used for hybridization are indicated.

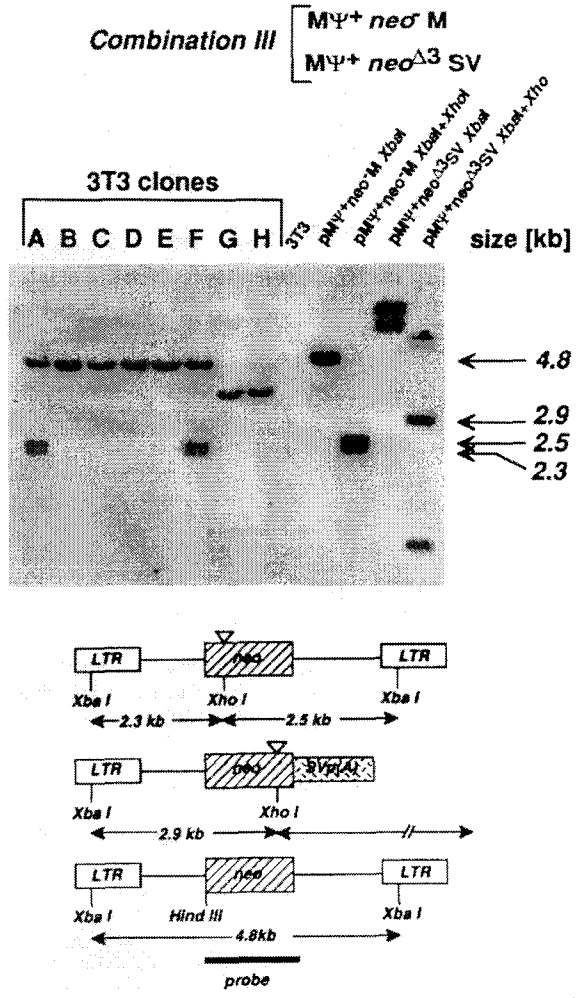

FIG. 5. Southern blot analysis of DNA from G418^r NIH 3T3 clones infected with virus from combination III (MΨ^+*neo*$^-$M/MΨ^+*neo*$^{\Delta 3}$SV). Digestions, electrophoresis, and hybridization were performed as described in the legend to Fig. 4. (Top) *Xba*I-*Xho*I digests. Lanes: A to H, 10 μg of DNA from eight different G418^r NIH 3T3 clones; 3T3, 10 μg of NIH 3T3 DNA. As controls, 10 μg of NIH 3T3 DNA mixed with 10 pg of pMΨ^+*neo*$^-$M DNA or with 10 pg of pMΨ^+*neo*$^{\Delta 3}$SV DNA was digested with *Xba*I alone or with *Xba*I and *Xho*I as indicated. The sizes of the respective fragments are indicated. (Bottom) Schematic structures of the mutant *neo* constructs and the putative recombinant *neo*$^+$ provirus. The positions of the *Xba*I, *Xho*I, and *Hin*dIII cleavage sites, the sizes of the expected fragments, and the probe used for hybridization are indicated.

pMΨ^+*neo*$^+$M (and, because of the small size difference, from *Xba*I-digested pMΨ^+*neo*$^-$M). This was the result obtained when DNA from seven of eight G418^r clones derived from combination I (MΨ^+*neo*$^-$M/MΨ^+*neo*$^{\Delta 3}$M) was digested with *Xba*I and *Xho*I (Fig. 4, top, clones B to H); one clone (clone A) gave rise to a smaller fragment. The distinctive patterns of *Hin*dIII fragments obtained from the proviral DNA in clones A to H show that they were derived from independent infections (data not shown). Note that in addition to the *neo*$^+$ recombinant provirus, most of the NIH 3T3 clones contained proviral DNA derived from the *neo*-minus (clone F) or *neo*$^{\Delta 3}$ construct (clones A, B, D, F, and G) or other *neo* sequences (clones A, B, and C). These additional provirus forms suggest that the NIH 3T3 cells were infected with more than one virus particle, at least one of which was able to give rise to the *neo*$^+$ recombinant provirus. Whether the unaltered mutant proviral sequences originate from viruses that contained only one type of the *neo* alleles or that failed to recombine during reverse transcription cannot be determined. The aberrant-sized fragment in clone A may

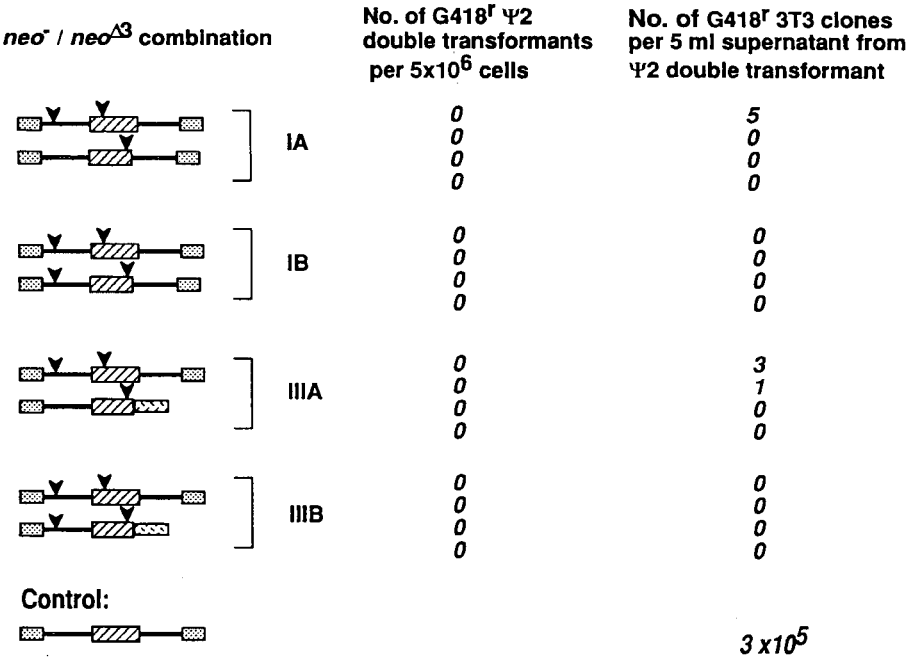

FIG. 6. Formation of recombinant *neo*$^+$ virus with Ψ^- vectors. The first column shows the number of G418^r cells in the double transformants carrying combinations of *neo*-minus and *neo*$^{\Delta 3}$ genomes. The second column shows the number of G418^r colonies produced after infection of NIH 3T3 cells with 5 ml of supernatant from the various double transformants. Four independent Ψ2 clones from each combination were analyzed.

have arisen from recombinations that generated an altered proviral form with a *neo*$^+$ allele and probably accounts for the low titer of *neo* virus produced after superinfection (Table 1).

Similar results were obtained when DNA from eight G418^r 3T3 clones derived from combination III (MΨ^+*neo*$^-$M/MΨ^+*neo*$^{\Delta 3}$SV) were analyzed (Fig. 5). In this experiment, six of eight G418^r 3T3 clones arose by homologous recombination as judged by the 4.8-kb fragment obtained after digestion with both *Xba*I and *Xho*I (Fig. 5, top, lanes A to F). This fragment is the same size as that produced by digestion of pMΨ^+*neo*$^-$M DNA with *Xba*I. Clones G and H are probably identical, as evidenced by the same *Hin*dIII digestion pattern (not shown). Each contains a single smaller recombinant provirus, possibly arising from either a deletion event in addition to the homologous recombination that resulted in a *neo*$^+$ allele or a nonhomologous recombination. In addition to the *neo*$^+$ recombinant provirus, clones A and F contain a MΨ^+*neo*$^-$M provirus, again indicating that these clones had been doubly infected.

In this combination, viral RNA derived from MΨ^+*neo*$^{\Delta 3}$ SV can neither complete reverse transcription nor integrate without recombination during the DNA negative-strand synthesis of reverse transcription. Since the frequencies of recombination obtained with RNA from combinations I and III are of the same order of magnitude (Fig. 3), we surmise that most or all of these recombinations took place during reverse transcription of the DNA negative strand. Southern analysis of DNA from G418^r 3T3 clones derived from two other independent Ψ2 double transformants from combination I and two from combination III confirms the results presented in this section (data not shown).

Absence of Ψ sequences leads to an increase in nonhomologous recombination. We reported earlier (30) that although *neo* RNAs lacking the Ψ site were poorly packaged into virions, the genomes that were included in the particles underwent frequent recombinations with the helper virus. Those recombinant viruses had often acquired the Ψ site from the helper virus, and many had undergone additional, nonhomologous recombinations. To test whether the frequency of nonhomologous recombination between the two replication-defective *neo* viruses is also high in the absence of the Ψ sequence, we made Ψ^- derivatives of the constructs shown in Fig. 1; these contain a 350-bp deletion of MoMLV sequences between nucleotides 212 and 563 (22). Ψ2 cells were sequentially transformed with DNA constructs as indicated in Fig. 6. The four types of Ψ2 double-transformant clones, designated IA, IB, IIIA, and IIIB, correspond to combinations I and III except for the absence of the Ψ site in one or both of the DNAs.

None of four independent Ψ2 double transformants of each combination were G418^r, indicating that none contained a functional *neo* gene (Fig. 6, column 1) and that therefore no recombination between the two mutant *neo* alleles had occurred. Virus contained in supernatants from Ψ2 clones carrying combinations IA and IIIA, in which only one of the recombination partners lacked the packaging sequence, were able to transduce G418^r, but at a low level. The number of *neo*$^+$ recombinants was about 10- to 20-fold smaller than the combinations in which both RNAs contained the packaging site (Fig. 3, combinations I and III). No recombinants could be detected when both recombination partners were Ψ^- (Fig. 6, combinations IB and IIIB).

Cellular DNA from one *neo*$^+$ recombinant NIH 3T3 clone derived from combination IA (3T3 #1), and from three recombinant NIH 3T3 clones derived from combination IIIA

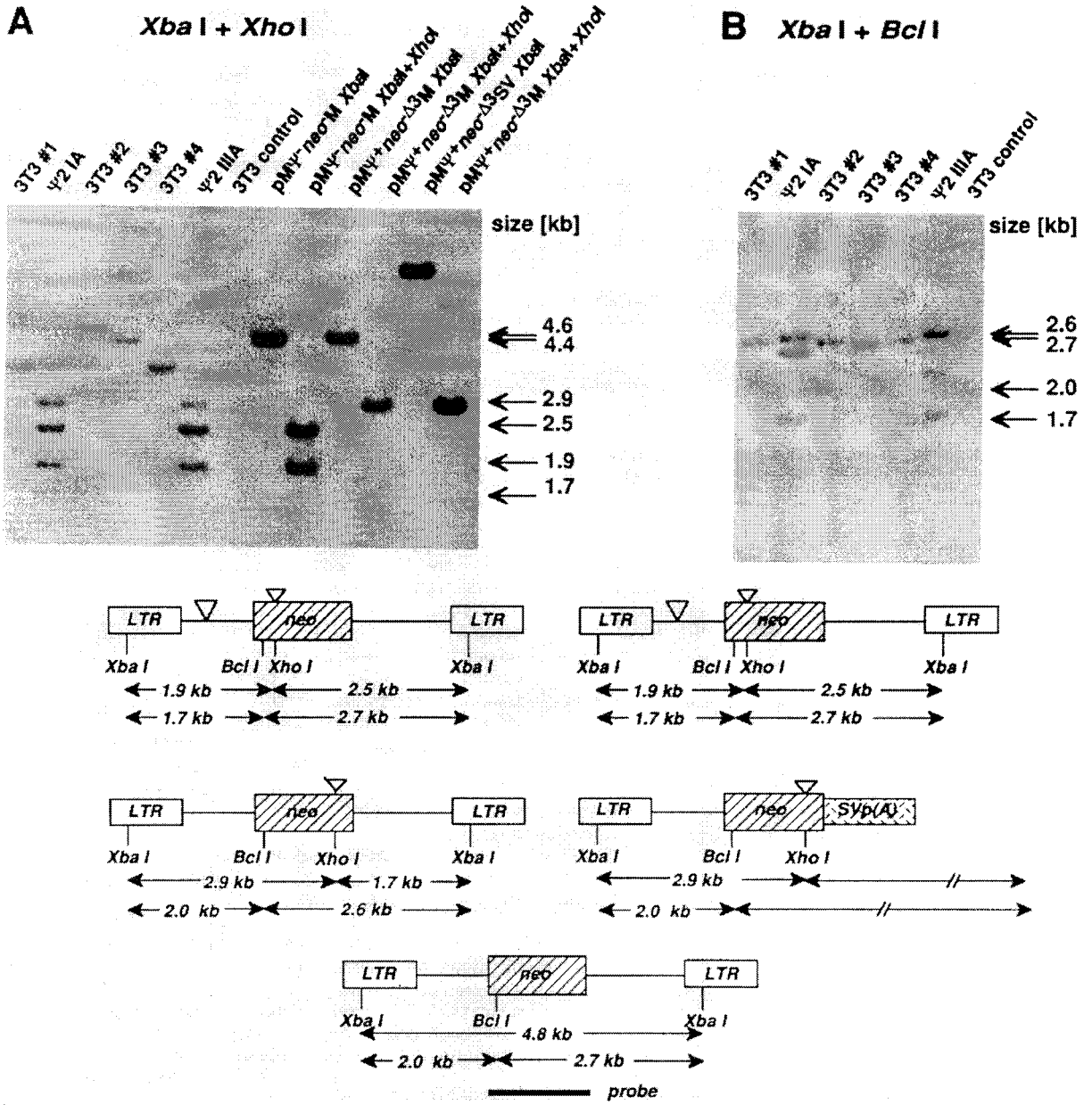

FIG. 7. Southern blot analysis of DNA from G418^r NIH 3T3 clones infected with virus from combinations IA and IIIA. High-molecular-weight DNA (10 μg) was digested to completion with enzymes as indicated. Electrophoresis and hybridization were performed as described in the legend to Fig. 4. (A) *Xba*I-*Xho*I digests. (B) *Xba*I-*Bcl*I digests. Lanes: 3T3 #1, DNA from G418^r NIH 3T3 clone infected with virus supernatant from Ψ2 IA; Ψ2 IA, DNA from Ψ2 double transformant cotransfected with pMΨ$^+$*neo*$^-$M plus pMΨ$^+$*neo*$^{\Delta 3}$M (combination IA); 3T3 #2 to 3T3 #4, DNA from three independent G418^r 3T3 clones infected with virus supernatant from Ψ2 IIIA; Ψ2 IIIA, DNA from Ψ2 double transformant, cotransfected with pMΨ$^+$*neo*$^-$M plus pMΨ$^+$*neo*$^{\Delta 3}$M (combination IIIA); 3T3, 10 μg of NIH 3T3 DNA. As controls, 10 μg of NIH 3T3 DNA mixed with 10 pg of pMΨ$^-$*neo*$^-$M DNA, with 10 pg of pMΨ$^+$*neo*$^{\Delta 3}$M DNA, or with 10 pg of pMΨ$^+$*neo*$^{\Delta 3}$SV DNA was digested with *Xba*I alone or with *Xba*I and *Xho*I as indicated. The sizes of the respective fragments are indicated on the right of the autoradiogram. (Bottom) Schematic structure of the mutant *neo* constructs and the putative recombinant *neo*$^+$ provirus. The positions of the *Xba*I, *Xho*I, *Hin*dIII, and *Bcl*I cleavage sites, the sizes of the expected fragments, and the probe used for hybridization are indicated.

(3T3 #2 to 3T3 #4), was analyzed by digestion with *Hin*dIII (data not shown) and by double digestion with *Xba*I and *Xho*I (Fig. 7A). If the *neo*$^+$ recombinant proviruses present in these clones were derived from a single homologous recombination event, as seen with the majority from combinations I and III (Fig. 4 and 5), they should have acquired the packaging sequence to produce a fragment of 4.8 kb (Fig. 7, bottom). However, double digestion with *Xba*I and *Xho*I yielded fragments which differed in size from 4.8 kb and from each other (Fig. 7A); in each case, however, the *neo*$^+$

recombinant proviruses had lost the *Xho*I restriction sites that mark the mutations (Fig. 7A, compare 3T3 #1–3T3 #4 with Ψ2 IA and Ψ2 IIIA). Digestion of the DNAs from these four transductants with *Hin*dIII showed that they were the product of independent proviral integrations (data not shown).

Further information about the structure of the recombinant genomes was obtained by double digestion with *Xba*I and *Bcl*I (Fig. 7B). *Bcl*I cuts once in the 5′ part of the *neo* gene, and double digestion with *Xba*I generates 5′- and 3′-specific fragments characteristic for the constructs and the recombinant proviruses (Fig. 7, bottom). Therefore, the 5′-specific fragment is 2.0 kb for Ψ^+ proviruses and 1.7 kb for Ψ^- proviruses, and the 3′-specific fragment is 2.7 kb for MΨ^+*neo*$^-$M and 2.6 kb for MΨ^+*neo*$^{\Delta 3}$M (Fig. 7, bottom; Fig. 7B, lanes Ψ2 IA and Ψ2 IIIA). A *neo*$^+$ recombinant provirus derived from a single homologous recombination should give rise to fragments of 2.0 and 2.7 kb after *Xba*I-*Bcl*I digestion (Fig. 7, bottom). However, as evident from the fragments observed in Fig. 7B, all four recombinant proviruses underwent additional nonhomologous recombinations at the 3′ end of their genome and also, in most cases, either additional homologous or nonhomologous recombinations at the 5′ end.

In summary, the results presented in this section confirm and extend our previous observation that deletion of the packaging sequence Ψ leads to an increased recombination frequency among genomes that are packaged (30). Here, we show that in the absence of Ψ in one of the mutant *neo* constructs, the frequency of *neo*$^+$ recombinants is reduced, but almost all of these recombinants underwent additional, mostly nonhomologous recombinations at other sites in their RNAs.

DISCUSSION

Genetic recombination is frequently observed among retroviruses. It occurs mostly between homologous sequences of exogenous or endogenous viruses (4, 7, 9, 10, 18, 28, 29, 32, 34–37), but can also occur between viral and cellular genes, leading to transduction of these cellular sequences. In the latter instances, the recombination often occurs within nonhomologous sequences or only very short stretches of homology (for a review, see reference 3).

A key characteristic of retroviruses is the dimeric nature of their genomes: two positive-strand RNA molecules are held together at or close to their 5′ ends (1, 2, 23, 24). Recombination among retroviruses appears to require copackaging of two genetically different RNA species into virions and a second round of infection (14, 34, 37). The copy choice model (8) and the displacement-assimilation model (17) for recombination both propose that high-frequency recombination takes place during reverse transcription of the heterodimeric RNA molecules. Alternative models which involve unintegrated viral DNA as targets for recombination have been proposed (reviewed in reference 16).

In this paper, we describe an experimental system to study the molecular mechanism of recombination between homologous retrovirus sequences by using MoMLV-based, replication-deficient vectors. These vectors each contain a mutant *neo* gene, with linker insertions in the 5′ or the 3′ region of the *neo* coding sequence. *neo*$^+$ recombinants were selected after one round of virus replication by their ability to confer G418 resistance to infected NIH 3T3 cells. The frequency of recombination between 560 bp of homologous *neo* sequences was in the range of 1×10^{-5} to 3×10^{-4} per virus replication cycle. This value is of the same order of magnitude as that of previous estimates obtained by measuring the transduction of *neo* mRNAs by replication-competent MoMLV (30). The frequencies obtained in our experimental system were significantly lower than the 10 to 30% that have been reported in earlier studies with avian or murine viruses (4, 18, 35–37). Most probably, multiple rounds of infection account for these higher estimates. The low frequency of single recombinations explains our inability to detect double recombinants ($<10^{-6}$), where two recombination events are required to generate *neo*$^+$ proviruses, for example with pair IV in Fig. 3. For such double recombinants to have arisen, one of the two recombination events would have had to occur within the 560 bp that separate the two *neo* mutations and the second event would have had to occur either within 130 bp of homology or a larger stretch of nonhomology 3′ of the *neo* sequences. Here, too, the occurrence of multiple rounds of virus replication in previous investigations (8) could explain the difference in our inability to detect multiple recombinations. In addition, a recent study by Hu and Temin (14) reported a recombination frequency of 2% per kilobase between spleen necrosis virus-based vectors per replication cycle. The 100-fold difference in recombination frequencies between their and our results may reflect differences in the organization and integrity of the RNA templates or in the ability of different reverse transcriptases to mediate recombination.

Deletion of the packaging sequence (Ψ) in one of the defective recombination partners decreases the number of recombinants about 10- to 20-fold. This result confirms our earlier finding (30) of a marked drop in recombination frequency if one of the viral RNAs cannot be packaged efficiently. However, despite the at least 10^3-fold-lower packaging efficiency previously determined for similar constructs (30), the recombination frequency fell by only 10- to 20-fold. This replicates our earlier observation (30) that when RNAs lacking Ψ are packaged, they undergo frequent recombinations.

From our analysis of the recombinant *neo*$^+$ provirus structures obtained with the constructs containing Ψ, we surmise that the majority (90%) result from homologous recombinations between the two markers. About 10% of the recombinants underwent additional nonhomologous recombinations or deletions (5 of a total of 42 recombinants analyzed). Any additional homologous recombinations that occurred 5′ or 3′ of the linker insertion mutations would not have been detected in our assay procedure. By contrast, when one of the recombination partners lacked the Ψ sequence, every recombinant provirus (four of four analyzed) had undergone additional nonhomologous recombinations.

Our experimental design allowed us to determine the stage in the virus life cycle at which the recombination took place. (i) If recombination between the two mutant *neo* constructs had occurred at the DNA level in the double transformants, these cells would have acquired a G418^r phenotype. However, none of the double transformants segregated G418^r cells, although they produced virus which could transduce a *neo*$^+$ phenotype in the next round of virus infection. Moreover, if gene conversion events between the two different types of integrated *neo* sequences were responsible for the appearance of recombinant viruses, combination IV should have produced *neo*$^+$ virus. Our data are most consistent with the view that recombination took place between the two defective viral RNAs after packaging into virion particles. (ii) Recombination must occur prior to integration of the

reverse-transcribed, double-stranded DNA into the NIH 3T3 host cell DNA. The same frequency of *neo*$^+$ recombinants was detected when one of the recombination partners lacked the 3′ LTR sequences necessary for integration as when both of the recombination partners contained 3′ MoMLV-derived sequences. (iii) Further support for identifying reverse transcription as the stage at which recombinants arise stems from our finding that both recombination partners must be copackaged into one virion. Thus, when each recombination partner was packaged into virions in separate cells, giving rise to viruses containing only homodimeric RNAs, no recombination occurred in the subsequent infections. This result is in agreement with results of earlier genetic experiments (34, 36, 37) and recent studies on recombination between spleen necrosis virus-derived retroviral vectors (14). The frequency with which two different RNAs are packaged into the same virion is not known because there is genetic but not physical evidence for copackaging. However, in our experiments, we assume that there is no bias in the packaging of the two *neo* RNA species, because all of the Ψ^+ constructs are identical at their 5′ ends, especially in the sequences which are involved in packaging of genomic RNA (22). Consequently, up to 50% of all the virion particles might be heterodimeric with respect to the type of RNA they contain. (iv) Our results suggest that recombination between the two copackaged RNAs can take place during synthesis of the first DNA strand (the negative strand), as predicted by the copy choice model (8). This conclusion follows because *neo*$^+$ recombinants are obtained even if one of the partners contains SV40 polyadenylation sequences at the 3′ end. In this case, completion of the DNA negative-strand synthesis cannot occur because the RNA lacking the characteristic viral sequences at the 3′ end cannot pair with the short DNA negative strand copied from the 5′ end of the template. Furthermore, synthesis of a DNA positive strand cannot be initiated because the *ppt* sequences are missing from the RNA with the SV40 poly(A) sequences (33). Therefore, in these instances, reverse transcriptase has to mediate the recombination event before completing the first (positive) DNA strand. Reverse transcriptase-mediated recombination may also occur during DNA positive-strand synthesis; however, we suspect that in our system recombination occurs predominantly during DNA negative-strand synthesis because the frequency of *neo*$^+$ recombinants is about the same whether or not recombination can occur during copying of either the negative or positive strand. Recently, template switching during reverse transcription has been observed in vitro (11a, 20).

The copy choice model predicts that only one recombinant provirus is generated from a heterodimer RNA (8). By contrast, the displacement-assimilation model supposes that two products are formed in the recombination event and that therefore the recombinant clones would be genetically heterozygous in that they contain parental and recombinant proviral DNA. Because our experimental design involves a drug selection for the recombinants and because cells carrying a parental or reciprocal proviral DNA would be eliminated by the drug selection, this prediction of the displacement-assimilation model could not be tested.

Overall, the results of our experiments are most consistent with the copy choice model proposed by Coffin (8). The recombination between two copackaged RNA molecules appears to take place after infection during the reverse transcriptase-mediated synthesis of the DNA negative strand, rather than during DNA positive-strand synthesis as proposed by the displacement-assimilation model (17). However, a recent study with spleen necrosis virus-based retrovirus vectors suggests that recombination can occur during the synthesis of both negative and positive strand DNA (15). It remains to be resolved whether this result reflects a difference in the mechanism of reverse transcription between spleen necrosis virus and MoMLV.

ACKNOWLEDGMENTS

We are grateful to all members of the Berg group for continuous discussions and encouragement of this project. We thank Patrick Brown and Ned Landau for critical comments on the manuscript.

H.S. is a fellow of the Cystic Fibrosis Foundation. This work was supported by Public Health Service grant GM-13235-24 from the National Institutes of Health to P.B.

REFERENCES

1. **Bender, W., Y.-H. Chien, S. Chattopadhyay, P. K. Vogt, M. B. Gardner, and N. Davidson.** 1978. High-molecular-weight RNAs of AKR, NZB, and wild mouse viruses and avian reticuloendotheliosis virus all have similar dimer structures. J. Virol. **25**:888–896.
2. **Bieth, E., C. Gabus, and J.-L. Darlix.** 1990. A study of the dimer formation of Rous sarcoma virus RNA and of its effect on viral protein synthesis *in vitro*. Nucleic Acids Res. **18**:119–127.
3. **Bishop, J. M., and H. Varmus.** 1984. Functions and origins of retroviral transforming genes, p. 999–1108. *In* R. Weiss, N. Teich, H. Varmus, and J. Coffin (ed.), RNA tumor viruses, 2nd ed. Cold Spring Harbor Laboratory, Cold Spring Harbor, N.Y.
4. **Blair, D. G., W. S. Mason, E. Hunter, and P. K. Vogt.** 1976. Temperature-sensitive mutants of avian sarcoma viruses: genetic recombination between multiple or coordinate mutants and avian leukosis viruses. Virology **75**:48–59.
5. **Chu, G., H. Hayakawa, and P. Berg.** 1987. Electroporation for the efficient transfection of mammalian cells with DNA. Nucleic Acids Res. **15**:1311–1326.
6. **Chumakov, I., H. Stuhlmann, K. Harbers, and R. Jaenisch.** 1982. Cloning of two genetically transmitted Moloney leukemia proviral genomes: correlation between biological activity of the cloned DNA and viral genome activation in the animal. J. Virol. **42**:1088–1098.
7. **Clavel, F., M. D. Hoggan, R. L. Willey, K. Strebel, M. A. Martin, and R. Repaske.** 1989. Genetic recombination of human immunodeficiency virus. J. Virol. **63**:1455–1459.
8. **Coffin, J. M.** 1979. Structure, replication, and recombination of retrovirus genomes: some unifying hypotheses. J. Gen. Virol. **42**:1–26.
9. **Elder, J. H., J. W. Gautsch, F. C. Jensen, R. A. Lerner, J. W. Hartley, and W. P. Rowe.** 1977. Biochemical evidence that MCF murine leukemia viruses are envelope (*env*) gene recombinants. Proc. Natl. Acad. Sci. USA **74**:4676–4680.
10. **Faller, D. V., and N. Hopkins.** 1978. T1 oligonucleotides that segregate with tropism and with properties of gp70 in recombinants between N- and B-tropic murine leukemia viruses. J. Virol. **26**:153–158.
11. **Feinberg, A. P., and B. Vogelstein.** 1983. A technique for radiolabeling DNA restriction endonuclease fragments to high specific activity. Anal. Biochem. **132**:6–13.

11a. **Firmenich, A., and P. Berg.** Unpublished data.

12. **Goodrich, D. W., and P. H. Duesberg.** 1990. Retroviral recombination during reverse transcription. Proc. Natl. Acad. Sci. USA **87**:2052–2056.
13. **Hartman, S. C., and R. C. Mulligan.** 1988. Two dominant-acting selectable markers for gene transfer studies in mammalian cells. Proc. Natl. Acad. Sci. USA **85**:8047–8051.
14. **Hu, W.-S., and H. M. Temin.** 1990. Genetic consequences of packaging two RNA genomes in one retroviral particle: pseudodiploidy and high rate of genetic recombination. Proc. Natl. Acad. Sci. USA **87**:1556–1560.
15. **Hu, W.-S., and H. M. Temin.** 1990. Retroviral recombination and reverse transcription. Science **250**:1227–1233.
16. **Hunter, E.** 1978. The mechanism for genetic recombination in

the avian retroviruses. Curr. Top. Microbiol. Immunol. **79**:295–309.
17. **Junghans, R. P., L. R. Boone, and A. M. Skalka.** 1982. Retroviral DNA H structures: displacement-assimilation model of recombination. Cell **30**:53–62.
18. **Kawai, S., and H. Hanafusa.** 1972. Genetic recombination with avian tumor virus. Virology **49**:37–44.
19. **Linial, M., and D. Blair.** 1984. Genetics of retroviruses, p. 649–784. *In* R. Weiss, N. Teich, H. Varmus, and J. Coffin (ed.), RNA tumor viruses. Cold Spring Harbor Laboratory, Cold Spring Harbor, N.Y.
20. **Luo, G., and J. Taylor.** 1990. Template switching by reverse transcriptase during DNA synthesis. J. Virol. **64**:4321–4328.
21. **Maniatis, T., E. F. Fritsch, and J. Sambrook.** 1982. Molecular cloning: a laboratory manual. Cold Spring Harbor Laboratory, Cold Spring Harbor, N.Y.
22. **Mann, R., R. C. Mulligan, and D. Baltimore.** 1983. Construction of a retrovirus packaging mutant and its use to produce helper-free defective retrovirus. Cell **33**:153–159.
23. **Murti, K. G., M. Bondurant, and A. Tereba.** 1981. Secondary structural features in the 70S RNAs of Moloney murine leukemia and Rous sarcoma viruses as observed by electron microscopy. J. Virol. **37**:411–419.
24. **Prats, A.-C., C. Roy, P. Wang, M. Erard, V. Housset, C. Gabus, C. Paoletti, and J.-L. Darlix.** 1990. *cis* elements and *trans*-acting factors involved in dimer formation of murine leukemia virus RNA. J. Virol. **64**:774–783.
25. **Rowe, W. P., W. E. Pugh, and J. W. Hartley.** 1970. Plaque assay techniques for murine leukemia viruses. Virology **42**:1136–1139.
26. **Smith, A. J. H., and P. Berg.** 1984. Homologous recombination between defective *neo* genes in mouse 3T6 cells. Cold Spring Harbor Symp. Quant. Biol. **49**:171–181.
27. **Southern, P. J., and P. Berg.** 1982. Transformation of mammalian cells to antibiotic resistance with a bacterial gene under control of the SV40 early region promoter. J. Mol. Appl. Genet. **1**:327–341.
28. **Stephenson, J. R., G. R. Anderson, S. R. Tronick, and S. A. Aaronson.** 1974. Evidence for genetic recombination between endogenous and exogenous mouse RNA type C viruses. Cell **2**:87–94.
29. **Stephenson, J. R., S. R. Tronick, and S. A. Aaronson.** 1974. Temperature-sensitive mutants of murine leukemia virus. IV. Further physiological characterization and evidence for genetic recombination. J. Virol. **14**:918–923.
30. **Stuhlmann, H., M. Dieckmann, and P. Berg.** 1990. Transduction of cellular *neo* mRNA by retrovirus-mediated recombination. J. Virol. **64**:5783–5796.
31. **Stuhlmann, H., R. Jaenisch, and R. C. Mulligan.** 1989. Construction and properties of replication-competent murine retroviral vectors encoding methotrexate resistance. Mol. Cell. Biol. **9**:100–108.
32. **Vogt, P. K.** 1971. Genetically stable reassortment of markers during mixed infection with avian tumor viruses. Virology **46**:947–952.
33. **Weiss, R., N. Teich, H. Varmus, and J. Coffin.** 1985. RNA tumor viruses: appendixes. Cold Spring Harbor Laboratory, Cold Spring Harbor, N.Y.
34. **Weiss, R. A., W. S. Mason, and P. K. Vogt.** 1973. Genetic recombinants and heterozygotes derived from endogenous and exogenous avian RNA tumor viruses. Virology **52**:535–552.
35. **Wong, P. K. Y., and J. A. McCarter.** 1973. Genetic studies of temperature-sensitive mutants of Moloney-murine leukemia virus. Virology **53**:319–326.
36. **Wyke, J. A., and J. A. Beamand.** 1979. Genetic recombination in Rous sarcoma virus: the genesis of recombinants and lack of evidence for linkage between *pol*, *env* and *src* genes in three factor crosses. J. Gen. Virol. **43**:349–364.
37. **Wyke, J. A., J. G. Bell, and J. A. Beamand.** 1975. Genetic recombination among temperature-sensitive mutants of Rous sarcoma virus. Cold Spring Harbor Symp. Quant. Biol. **39**:897–905.